IEEE Access
Multidisciplinary ⋮ Rapid Review ⋮ Open Access Journal

Received December 30, 2020, accepted January 10, 2021, date of publication January 18, 2021,
date of current version January 25, 2021.

Digital Object Identifier 10.1109/ACCESS.2021.3052315

Protection Scheme using Wavelet-Alienation-Neural Technique for UPFC Compensated Transmission Line

BHUVNESH RATHORE[1], OM PRAKASH MAHELA[2], (Senior Member, IEEE), BASEEM KHAN[3], (Member, IEEE), AND SANJEEVIKUMAR PADMANABAN[4], (Senior Member, IEEE)

[1]Department of Electrical and Electronics Engineering, MBM Engineering College, Jodhpur 342011, India
[2]Power System Planning Division, Rajasthan Rajya Vidyut Prasaran Nigam Ltd., Jaipur 302005, India
[3]Department of Electrical and Computer Engineering, Hawassa University, Hawassa 05, Ethiopia
[4]Centre for Biology and Green Engineering, Department of Energy Technology, Aalborg University, 6700 Esbjerg, Denmark

Corresponding author: Baseem Khan (baseem.khan04@ieee.org)

ABSTRACT Fault analysis (detection, classification and location) of transmission network is of great importance in power system. A Wavelet-Alienation-Neural (WAN) technique has been developed for the fault analysis of Unified Power Flow Controller (UPFC) compensated transmission network. The detection and classification of various outages are accomplished by alienation of wavelet based approximate coefficients computed from current signals. The precise location of faults is carried out by an Artificial Neural Network fed from estimated approximate coefficients computed from voltage and current signals of the same quarter cycle. The robustness of the algorithm is proved with the case studies of varying fault locations, sampling frequency, system parameters, effects of noise, fault incipient angle, different control strategies and fault path impedances.

INDEX TERMS Fault detection, fault classification, fault location, unified power flow controller (UPFC).

I. INTRODUCTION

In power engineering, the transmission system must be reliable and efficient for making the power system stable and having good economic condition. This can only be achieved by high speed protection schemes against transmission line faults. However, these protection schemes are influenced by the compensation devices which are used for the enhancement of power transfer capability and the power quality. Such devices include Static Synchronous Series Compensator (SSSC), Static Synchronous Compensator (STATCOM), Unified Power Flow Controller (UPFC), Static Var Compensator (SVC), etc. Among these devices, UPFC, which combines the features of the STATCOM and SSSC, has versatile performance and complex structure. The existence of compensating device in the outage condition affects the current and voltage values at the point of relay, which may lead to over-reach or under-reach, in case of conventional distance protection. This is due to change in apparent impedance, affected through the voltage and current signals injected by UPFC. Hence there is a need to explore the capability of signal processing and artificial intelligence techniques, which can overcome the limitations of conventional distance protection scheme.

A variety of protection techniques are introduced by the different researchers for UPFC-compensated network. A performance study of distance protection on UPFC-integrated network, including modelling of UPFC, its control strategy and its integration into system, was carried out by Zhou, *et al* [1]. A modified distance protection for UPFC-compensated power network is presented by Dash, *et al.* [2]. An adaptive and modified version of distance protection scheme, considering influence of UPFC, was proposed in [3]. In [4], an adaptive distance relay scheme for wind and UPFC connected parallel transmission lines is reported. Fault classification in transmission lines, equipped with FACTS devices, using decision tree was introduced in [5]. Samantaray, *et al.* [6], introduced a differential equation depended technique for fault location on UPFC-compensated system, which makes use of synchronized phasor measurements. Ahsaee and Sadeh [7], proposed a technique for locating the faults on transmission network with UPFC compensation, based on the synchronized data. A decision tree-induced fuzzy rule based

The associate editor coordinating the review of this manuscript and approving it for publication was Akshay Kumar Saha.

technique is utilized to develop differential relaying for transmission lines, integrated with wind farm and UPFC [8]. Stockwell-transform (S-transform), which has combined features of short-time Fourier and wavelet transform, had been extensively utilized in the field of line protection. Tripathy *et al*. [9] & [10] has presented S-transform based protection algorithm for UPFC based transmission system. Features extracted, using S-transform, are fed to Support vector machine (SVM), to protect a transmission line, compensated by UPFC in [11]. A SVM based fault location algorithm for UPFC connected transmission network, which makes the use of features extracted from S-transform of current signals, was proposed by Moravej *et al.*, [12]. A protection algorithm for UPFC compensated double-circuit transmission lines had been proposed, based on the differential relaying scheme making use of the fast-discrete S-transform [13]. A novel protection technique based on Wavelet Transform for UPFC connected transmission line is presented by Goli *et al.* [14]. For detecting and classifying the fault in UPFC integrated transmission network, a wavelet entropy based technique is introduced by Zonkoly and Desouki [15]. For the wind DG and UPFC integrated tapped transmission network, a wavelet based differential protection technique is introduced in [16]. An alienation (AL) coefficient based network protection technique using local bus data, is developed by Masoud and Mahfouz [17]. The wavelet transform based AL coefficients, which were obtained from local buses, are utilized to develop the network protection method by Gafoor, *et al.* [18]. References [19], [20] and [21] presented transmission line protection schemes, which utilize wavelet depended alienation technique. A technique using current features evaluated using Wigner distribution function (WDF) and AL coefficient is implemented to protect the transmission line (TL) [22] and grid in the availability of photo voltaic [23] and renewable energy (RE) sources based hybrid grid [24]. This protection scheme has the advantage of low fault recognition time. A protection scheme for hybrid system based on FDOST has been introduced in [25].

In this research work, a WAN based protection scheme has been proposed for UPFC compensated transmission system. It aims at achieving fault detection and classification within quarter cycle time i.e. within 5ms, along with fault location making use of minimum sample time features using ANN. The contributions of the proposed algorithm are as follows:

- An absolute protection scheme for transmission system achieving fault detection, fault classification and fault location is proposed.
- This protection scheme can detect the fault in least possible time which is < 5 ms.
- This makes use of minimum amount of data, available after the fault incidence, (i.e. of quarter cycle time) for fault detection, classification and also for fault location.
- This protection scheme is robust against maximum number of fault environments such as variation in fault location, FIA, fault impedance, UPFC control strategy, system parameters, line length, and noisy environment.

The paper is structured in 10 segments. In Segment 2, discussed the protection challenges for FACTS compensated transmission systems and the proposed system, its parameters and simulation details in segment 3. Segment 4 included proposed protection strategy and its demonstration for fault analysis is given in segment 5. Segment 6 covered the case studies utilized in this work. Prediction of fault location is presented in segment 7. The effect of UPFC absence on the proposed technique is shown in segment 8 and comparison with literature schemes has been presented in segment 9, followed by the conclusion in segment 10.

II. PROTECTION CHALLENGES IN THE FACTS COMPENSATED TRANSMISSION LINES

For protection of transmission lines Distance Relays are used which works on the basis of apparent impedance measurement from the fault point. Although FACTS devices provides various advantages, but they have negative impacts also on the relay functioning, which is detailed in following sections

A. IMPACT OF SERIES FACTS DEVICE: SSSC

The impact of SSSC on transmission line protection system can be summarized as follows:

- SSSC can be installed at the substation or at the middle of the line as midpoint compensator. SSSC affects the protection system depending upon its location. SSSC does not affect the line protection system if not present in the fault loop.
- SSSC is connected in series with the transmission line and works in capacitive and inductive mode of operation so it shows both over-reaching and under-reaching effects at relay end.
- The problem of voltage inversion can also occur if in the fault loop because of SSSC presence, capacitive reactance is greater than the inductive reactance
- The location of voltage transformer (VT) is also affected by presence of SSSC in the system. For least impact of SSSC on distance protection, Voltage Transformer in front of SSSC is the preferred location

B. IMPACT OF SHUNT FACTS DEVICE: STATCOM

The impact of STATCOM on transmission line protection system can be summarized as follows:

- It affects the distance relaying by altering the apparent impedance measurement resulting into overreaching and under reaching of the relay.
- STATCOM presence in the transmission system results in increasing relay operating time from less than one cycle to 5–7 cycles.
- In case of unsymmetrical fault occurrence on STATCOM compensated system, faulty phase voltage experience under voltage effect while healthy phases' voltages increases due to overcompensation by STATCOM. As a result, healthy phase may experience high line current and the overcurrent relay may result it as a fault.

C. IMPACT OF COMPOSITE DEVICE: UPFC

UPFC is the combination of SSSC (a series device) and STATCOM (a shunt device), so it affects the protection system in more complex manner. UPFC can consume both active power and reactive power. The effect of UPFC presence on line protection are as follows:

- Among various FACTS devices, the use of unified power flow controller (UPFC) in power system network is constrained due to its dynamic behaviour as UPFC is generally observed to create problems pertaining to stability and functionality of the protection systems. As the third generation FACTS device, Unified Power Flow Controller (UPFC) is an effective means to control the state of the power grid. It only needs to change the control rules to realize shunt compensation, series compensation, phase shifting and voltage regulation.
- UPFC has greater influence on the apparent resistance; this is due to the active power injection and consumption by both SSSC and STATCOM.
- When the UPFC injects reactive power into the system, it is operated like a series capacitor and the apparent impedance decreases, in this case Mho relay overreaches. When it consumes reactive power from the system, it is operated like a series inductance and the apparent impedance increases and Mho relay overreaches.
- If UPFC presents in the fault loop, it will affect both the steady state and transient components in the measured voltages and currents, consequently impact the apparent impedance seen by the distance protection.
- Load encroachment and power swing.

Analytically, it can be explained as follows:

In transmission system without FACTS device, for an LG fault, the apparent impedance for distance relay can be calculated as:

$$Z = \frac{\mathrm{VR}}{\mathrm{IR} + \mathrm{IR0}\frac{\mathrm{Z0}-\mathrm{Z1}}{\mathrm{Z1}}} = \frac{\mathrm{VR}}{\mathrm{Irelay}} \tag{1}$$

where, Zo represents zero sequence impedance, Z1 is positive sequence impedance, VR & IR are phase voltage and current at relay point; IR0 is zero sequence phase current and I_{relay} is relaying current.

For system with STATCOM, the apparent impedance seen by the relay can be expressed as:

$$\mathrm{Z} = \mathrm{mZL_1} + \frac{\mathrm{Ish}}{\mathrm{Irelay}}(\mathrm{m}-0.5)\,\mathrm{ZL1} + \mathrm{Rf}\frac{\mathrm{If}}{\mathrm{IR}} \tag{2}$$

where, m represents fault location from the relay to fault point in per unit of the total line length, ZL_1 is positive sequence components of the line impedance, I_{sh} is sequence current of the shunt device, IR is zero sequence current, Rf is fault resistance, and If is sequence current in the fault resistance.

From this, it can be clearly observed that it has two parts: positive sequence part from relay point to fault point which is what relay is to measure and the second is due to shunt current I_{sh} injected by STATCOM.

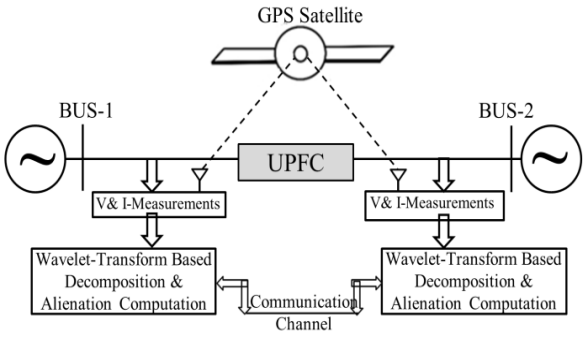

FIGURE 1. UPFC-Compensated transmission system.

If this conventional distance relay is applied to the transmission system with UPFC, the apparent impedance seen by this relay can be expressed as

$$\mathrm{Z} = \mathrm{mZ1} + \frac{\mathrm{Ish}}{\mathrm{Irelay}}(\mathrm{m}-0.5)\,\mathrm{Z1} + \frac{\mathrm{I0sh}}{\mathrm{Irelay}}(\mathrm{m}-0.5) \times (\mathrm{Z0}-\mathrm{Z1}) + \mathrm{VpqIrelay} + \mathrm{IfIrelayRf} \tag{3}$$

For system with UPFC, the apparent impedance seen by the relay has three parts: positive sequence impedance from relay point to fault point, which is what relay is to measure: the second is due to impact of UPFC on the apparent impedance, which can be further divided into two parts: one results from the shunt current I_{sh} injected by STATCOM and another is the impact of the series voltage V_{pq} injected by SSSC: the last part of the apparent impedance is due to the fault resistance.

III. PROPOSED SYSTEM AND ITS PARAMETERS

The UPFC-compensated transmission system, shown in Fig. 1, has been simulated using MATLAB/ SIMULINK software and within it by using simpowersystem toolbox. The rating of transmission line (TL) is 500kV, 60 Hz and UPFC is placed at mid of the TL. The parameters required for simulation of each block, has been illustrated in Table-1 [11], like for AC sources, line length, transmission line parameters and UPFC (STATCOM and SSSC) compensation device. For computation of fault index and decision making algorithm, program has been written in the editor of MATLAB and analysis has been done for various case studies by exporting data from SIMULINK (by simulating model every time for new case and generating various data). For case studies, the required simulation strategy can be explained by following steps:

- The type of fault can be varied from the fault block used in the model by selecting the type of faulty phase.
- The fault location can be varied by connecting the fault block between transmission line blocks of different length.
- The fault impedance can be changed in the fault block using 'Fault Resistance' attribute.
- Fault incidence angle variation can be reflected by converting the angle into time and keeping it as fault incidence time.

TABLE 1. System parameters.

AC Sources (500 kV)	
Bus-1 & Bus-2 Source Impedance	Z_S= 2.9142 + j29.4117 Ω
Transmission Line (300 km)	
Resistance (Ω/km)	R_0=0.3864 R_1=0.0254
Inductance (H/km)	L_0=4.1264 x 10^{-3} L_1=9.337 x 10^{-4}
Capacitance (F/km)	C_0=7.751 x 10^{-9} C_1=12.74 x 10^{-9}
UPFC	
Shunt Converter: Nominal value of Power in MVA Voltage (Coupling Transformer) kV	 100MVA 500/15
Series Converter: Nominal value of Power in MVA Injection of Voltage in kV Voltage (Coupling Transformer) kV	 100MVA 50 kV (10%) 12.5/12.5

- For considering effect of noise contamination, current signals are contaminated with noise of different SNRs by using a command 'awgn' for white Gaussian noise..
- For Load switching effect, inductive and capacitive load blocks are connected at bus-2 with ratings as 10 % and 20 % of rated power.
- For considering sampling frequency effect, signals are recorded with different sampling frequencies from simulation model by varying attributes of 'To workspace' block.

IV. PROPOSED PROTECTION STRATEGY

For the proposed algorithm ANN and Wavelet Transform (WT) have been used as application tools. The contributions w.r.t. ANN model and WT are as follows:

a. The Wavelet Transform is conceptually the modification of Fourier analysis (STFT) with variable window size. Since the fault transients are non-stationary in nature, therefore it is an efficient tool for their analysis in time-frequency domain. It helps in localizing the high frequency transient with respect to time. For analysis the window or vector size varies with frequency of signal, to be analyzed. At high frequencies the window size gets reduced while for lower frequencies, its width increases to collect more information. The wavelet transform have got a special feature of magnifying the difference/ change in data points (like difference in the magnitude of healthy and faulty signals), which has been signified by obtaining approximate coefficients and utilising them for computing alienation coefficients (AL).

b. Artificial neural network is a parallel distributed processor that has a natural propensity for storing experiential knowledge and making it available for use. ANN has got excellent pattern recognition capabilities which could be helpful for classifying/ prediction problems in real time scenario. For prediction of fault location, ANN has been used as regression model. For which, firstly it has been trained with a wide range of case studies data, which has established a pattern/ regression model/ axis between input data and fault location and then this trained ANN model has been utilised for prediction of fault location for new input data points, by matching the new input data points w.r.t. regression model. The input to NN will be the approximate coefficients, of each phase voltage and current signal, computed over the span of quarter cycle, from both the ends of the line. Moreover, neural network has following advantages:

- Feed forward neural networks have a fixed computation time.
- Computation Speed is very high, as a result of the parallel structure.
- Fault tolerant because of distributed nature of network knowledge.
- Learns general solutions of presented training data.
- If an explicit mathematical model is not required, then the network can be 'programmed' in a fraction of the time required for traditional development.
- It can learn from noisy and incomplete data, only the solution will just be less precise.
- Ability to generalize to situations not taught to network previously.

In this section, WAN technique and protection (fault detection, classification and location) strategy have been discussed.

A. WAN TECHNIQUE

For the proposed algorithm, wavelet transform and alienation coefficients are used for fault detection and classification while wavelet transform and neural network are used for fault location, thus it is termed as Wavelet-Alienation-Neural (WAN) Technique. For fault detection and classification, approximate coefficients based alienation (AL) coefficients are utilised, which can be computed in following manner by equation (4) and (5):

$$A_a = 1 - r_a^2 \tag{4}$$

where, A_a is defined as AL coefficient and correlation coefficient is represented by r_a, which is computed as follows by (5)

$$r_a = \frac{N_s\left(\sum x_a y_a\right) - \left(\sum x_a\right)\left(\sum y_a\right)}{\sqrt{\left[N_s \sum x_a^2 - \left(\sum x_a\right)^2\right]\left[N_s \sum {y_a}^2 - \left(\sum y_a\right)^2\right]}} \tag{5}$$

where, **Ns** represents the number of samples (in a quarter cycle), $\mathbf{x_a}$ represents array of low frequency A-1 coefficients obtained from window-$\mathbf{W_0}$, and $\mathbf{y_a}$ represents array of A-1 coefficients obtained from window-$\mathbf{W_{-1}}$, (T = 16.67ms).

B. FAULT DETECTION STRATEGY

The current signals are measured from both the bus terminals and for recording they are sampled with the frequency of 1.92 kHz. The GPS clock provides time signature to the samples measured at any bus, such that when they are communicated to another bus, they will be analysed accurately

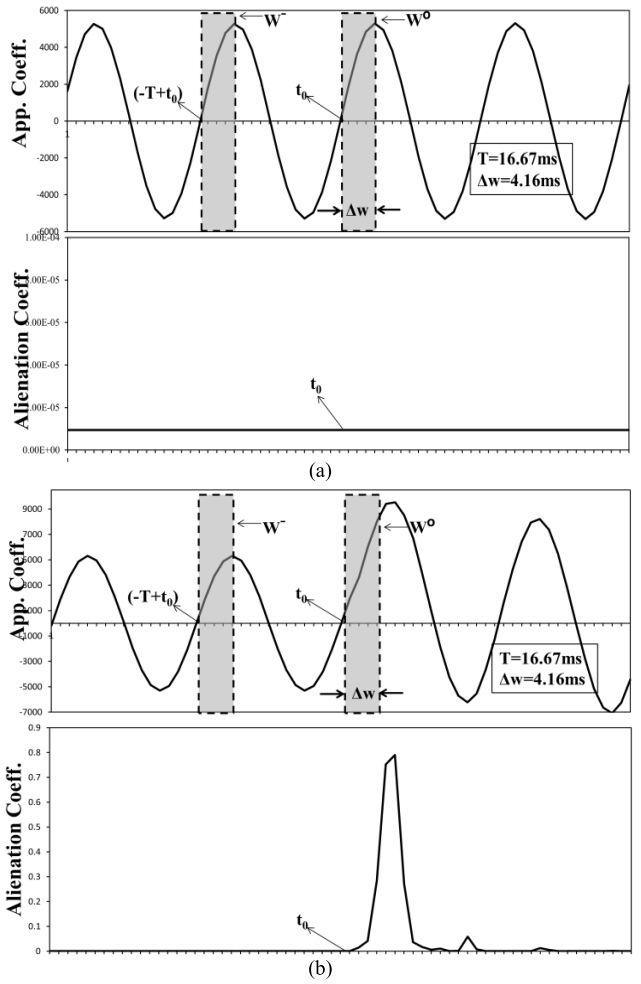

FIGURE 2. Computation of AL Coefficients by comparing windows (a) Without Fault (b) With Fault at t_0.

w.r.t. the time and an accurate decision can be made regarding fault diagnosis. For extracting approximate coefficients, current signals are analyzed by WT with db2 as mother wavelet which is chosen after trial and error performing with different wavelets.

These signals are computed/sampled over a varying window of quarter cycle. For calculating the AL coefficients, current window's ($\mathbf{W}_0$) approximate coefficients are compared with previous window's ($\mathbf{W}_{-1}$) coefficients, which are separated by a cycle, as illustrated in Fig. 2. Fault Index (FI) is computed by summing up the coefficients of alienation obtained from both the buses. The value of AL coefficients and FI would remain at zero due to the similarity of captured/compared signals/windows, which is the condition for healthy signals. Because of the differences in the recorded signals under faulty condition, the AL coefficients and FI would achieve a non-zero/finite value. For detecting the fault, the obtained FI is compared with the fault threshold (F-TH) value i.e. 0.2. Thus, for fault detection FI value is monitored, when it, for a particular phase, rises above the F-TH, then it indicates fault occurrence/incidence, hence it acts as a numerical relay for fault detection.

C. FAULT CLASSIFICATION STRATEGY

Subsequent to the fault detection, faults can also be classified by the same FI only. After fault detection, it is observed that for which and how many phases, the FI value is greater than the F-TH, based on that fault type identification can be done, using following decision rules:

- If FI of only single phase exceeds the F-TH, then it is identified as L-G fault. Further, based on which phase is faulty among LG faults also, it can be classified as AG, BG or CG fault.
- If FI value of any two phases rises beyond the F-TH, then it can be classified as a two-phase fault and also based on type of faulty phase, it can be classified as AB, ABG, BC, BCG, AC or ACG fault. Now, there is another criteria required for discrimination two-phase fault whether with or without ground. For this, a zero sequence current depended ground fault index (G-FI) has been introduced. It is computed by accumulating the approximate decomposition of zero sequence current with a varying window over the span of quarter cycle. This resultant G-FI is compared with a new threshold, which is termed as ground fault threshold (GF-TH = 500) for the discrimination between LL and LLG faults.
- If for all the three-phases the FI value is greater than the F-TH, then the fault is classified as a three-phase fault or ABCG fault.

D. FAULT LOCATION STRATEGY

Location of fault is estimated with the help of Artificial Neural Network (ANN) which has been discussed in this section.

1) ANN Selection/ Structure

Suppose the input $x = [x_1, x_2, x_3 \ldots x_n]$ be a n-dimensional vector which is connected to the neurons through weighted synaptic links represented as $w = [w_1, w_2, w_3, \ldots w_n]$. The output of each neuron is the weighted sum of each input and is given as:

$$z = \sum_{i=1}^{n} w_i x_i + b \tag{6}$$

which can be written as:

$$Z = \mathrm{W}^{\mathrm{T}}\mathrm{X} \tag{7}$$

where b is a bias term

Thus, the synaptic operation assigns a relative significance to each incoming input signal, x_i, according to the past experience stored in w_i. This provides a linear mapping from n-dimensional neural input space, X, to the one-dimensional space. The output is passed through an activation function whose output is the final output of the neuron and can be written as:

$$y = \phi(Z) \tag{8}$$

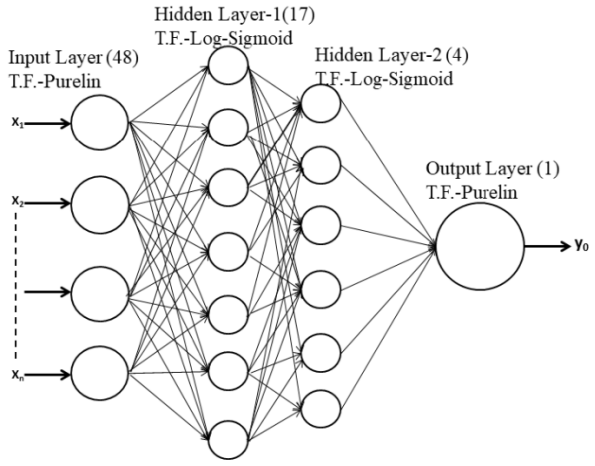

FIGURE 3. ANN Structure.

The ANN used is Multi-layer perceptron model with Levenberg-Marquardt optimization method and use backpropagation supervised training. Such option is typical when applying ANN to power system studies. It consists of nonlinear differentiable transfer functions. A three-layer (i.e. two-hidden-layer) feed forward neural network has been used, which can fit any input-output relationship given enough neurons in the hidden layer. Layers which are not output layers are called hidden layers. The input and output have sizes of 0 because the network has not yet been configured to match our input and target data. This will happen when the network is trained. NN toolbox of MATLAB is used for developing the model. The ANN Structure has been depicted in Fig. 3.

2) ANN input

As a first step in any prediction technique, feature extraction is used to reduce the dimension of the raw data and extract useful information in a concise form. For the ANN considered here, this process leads to a considerable reduction in size of the network, thereby significantly improving the performance and speed of the training process. The technique adopted here for feature extraction is the one based on time domain frequency decomposition of voltage and current waveforms i.e. Wavelet Transform.

The input to NN will be the approximate coefficients, of each phase voltage and current signal, computed over the span of quarter cycle, from both the ends of the line. Thus, the total number of inputs will be computed as: for 2-buses with 3-phase voltage and 3-phase current signals and 4 coefficients for each $= 2^*(3+3)^*4 = 48$ coefficients.

3) ANN Training

The back-propagation learning rules are used to adjust the weights and biases of networks so as to minimize the sum squared error of the network. This is achieved by continually changing the values of the network weights and biases in the direction of steepest descent with respect to error. The back-propagation training may lead to a local rather than a global minimum. The local minimum that has been found may be satisfactorily, but if it is not, a network with more layers and neurons may do a better job. However, the number of neurons or layers to add may not be obvious. MLP architecture has been decided by trying varied combinations of number of hidden layers, number of nodes in a hidden layer etc. and selecting the architecture which has a better generalizing ability amongst the tried combinations.

TABLE 2. Simulation parameters for training ANN.

S.No.	Attributes	Parameters
1	No. of Fault Locations	30 (for 300 km line, at a steps of 10 kms)
2	Types of Faults	10 (AG, BG, CG, AB, BC, AC, ABG, BCG, ACG, ABCG)
3	Fault Impedances	4 (0, 5,10,15 Ω)
4	Fault Incidence Angle	6 (0, 30, 60, 90, 120, 150)
5	Total number of data sets obtained	30*10*4*6 = 7200
6	Training Data Sets	(70%) 5040
7	Validation Data Sets	(15%) 1080
8	Testing Data Sets	(15%) 1080

The training of utilized ANN has been performed through providing 48 approximate coefficients of post-fault 3-Φ voltage and current data, of quarter time period. The samples are automatically divided into training, validation and test sets. The training set is used to teach the network. Training continues as long as the network continues improving on the validation set. The test set provides a completely independent measure of network accuracy. The details of the simulated data, used for training are given in Table-2.

The MATLAB neural network toolbox is used for training the networks. The function 'trainlm' is used, which converges in lesser time as well as in few epochs compared to the training function 'trainbpx', of the neural network toolbox. Each epoch or training iteration represents the presentation of the set of training vectors to a network and the calculation of new weights and biases. The training function 'trainlm' uses Levenberg–Marquardt optimization, which is a more sophisticated method compared to the gradient descent approach, but requires more memory. The error goal for all the all the cases is chosen to be 0.001%.

The learning parameters for all the cases are kept the same. The training parameters used in this work are:

a. Momentum: 0.9.
b. Learning rate: 0.01.
c. Desired error (minimum error): 1×10^{-6}
d. Maximum number of iterations: 10000.
e. Activation function: Log-sigmoid and Purelin

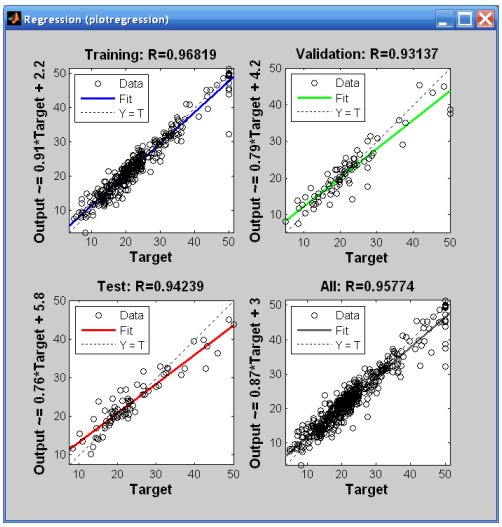

FIGURE 4. Regression Plot for ANN training.

To achieve a lower value of Mean square error and higher regression index, the number of neurons was changed and these values are checked for each iteration. If the performance on the training set is good, but the test set performance is significantly worse, which could indicate over fitting, and then reducing the number of neurons can improve results. If training performance is poor, then the number of neurons is to be increased. For a perfect fit, the regression plot data should fall along a 45 degree line, where the network outputs are equal to the targets. From Fig.-4 it is depicted that the fit is reasonably good for all data sets, with R values for following case of 0.93 or above. If even more accurate results were required, the network is retrained. This will change the initial weights and biases of the network, and may produce an improved network after retraining. It is to be noted that although the ANN locates the fault accurately, there are small fluctuations in the ANN output and in practice this cannot be avoided. The error in locating the exact fault can be expressed as a percentage of the length of the transmission line and is given by:

$$\%\varepsilon = \frac{|NN\ Distance - Actual\ Distance|}{\text{Length of line}} \qquad (9)$$

4) ANN Testing

The ANN testing has been done for new inputs of different fault locations. The maximum error in locating the exact fault is found to be less than 1%. The network reached the error goal in about 1000 epochs and 400 s of training time. This suggests that the algorithm could quickly learn different network conditions if encountered. The network tested correctly for about 96% of the cases, which it had not seen before. The correct testing indicates that the ANN has generalized and not just memorized the patterns. The ANN based algorithm is found to be an accurate fault locator in the presence of different fault distances, fault inception angle, and fault resistance. Taking into account that in some cases, the distances are spaced just by 1% apart, the ANN-based algorithm has been able to identify the faults accurately for the cases not seen before.

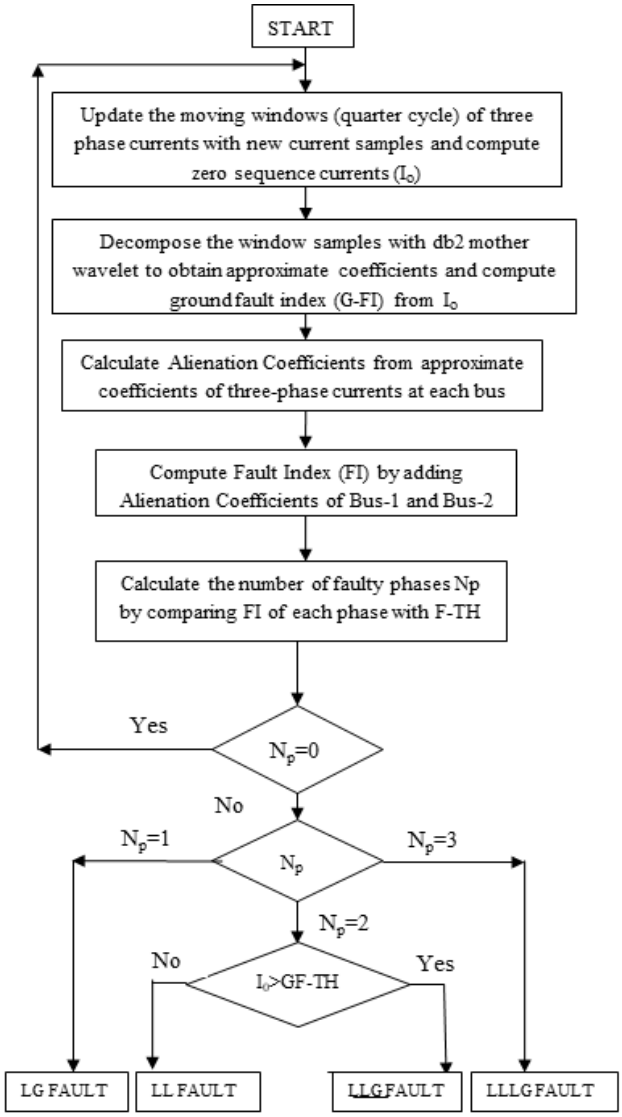

FIGURE 5. Flowchart of the proposed algorithm.

The flowchart for the proposed algorithm can be illustrated in Fig. 5.

E. IMPLEMENTATION FOR REAL-Time/PRACTICAL SYSTEM

To implement the proposed algorithm for real-time/ practical system following points are to be considered:

- For implementation of proposed algorithm in real world, it will require a computer with high-speed processor and the communication channels among various stations of a power system, which are well established in the modern power system, along with phase measurement units (PMUs), where the sampled signals are synchronized

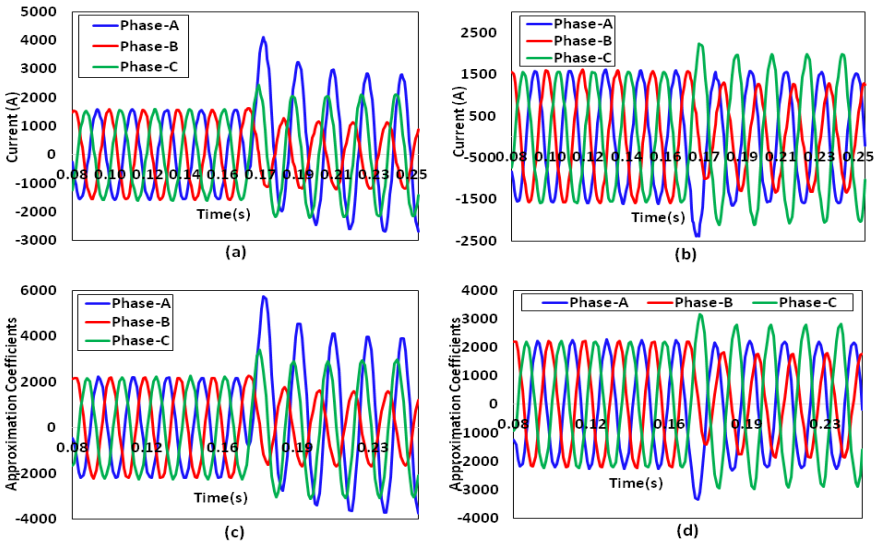

FIGURE 6. Plots for Current Signals and Approximate coefficients (App. Coeff.) (a) Bus-1 Current Signals (b) Bus-2 Current Signals (c) Bus-1 App. Coeff (d) Bus-2 App. Coeff.

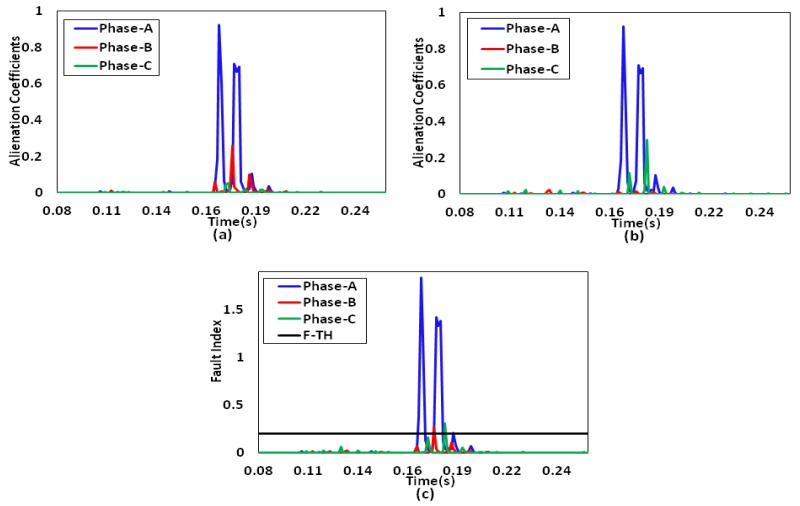

FIGURE 7. Demonstration for diagnosis of AG-fault (a) Bus-1 AL Coefficients (b) Bus-2 AL Coefficients (c) FI plot w.r.t. time.

with a GPS clock. Thus, the proposed algorithm does not require any additional infrastructure in the scenario of modern power system.

- The proposed protection method would be working online when to be used for real time/ practical system. For online system, this algorithm will be continuously running/ working every time by computing fault index for each instance of current signal and when it will get fault index value greater than the threshold at the same instant it will send trip signal to the circuit breaker.
- In modern power system, since the computers, used in the Numerical protection, has processors with of latest generation (i7) for having high computation ability, huge memory capacity (1TB) and high speed or (few GHz), which takes negligible amount of time for huge and complex computation.
- Since computation of fault index requires both the bus data, thus if there will be delay with remote end data then it could result into an incorrect value of fault index for a particular time instant, and hence incorrect decision will be made for fault diagnosis like delayed or no detection of fault and incorrect classification of fault.
- Before starting fault analysis, the communicated signals (with GPS time signature) are checked for synchronization error by computing differential sum of currents which should be zero for healthy case only if the currents samples of same time instances have been added otherwise it will be non-zero. In case if any synchronization error is found, it will be compensated by adding or subtracting corresponding time difference to the communicated data to make it suitable for utilization in decision making.

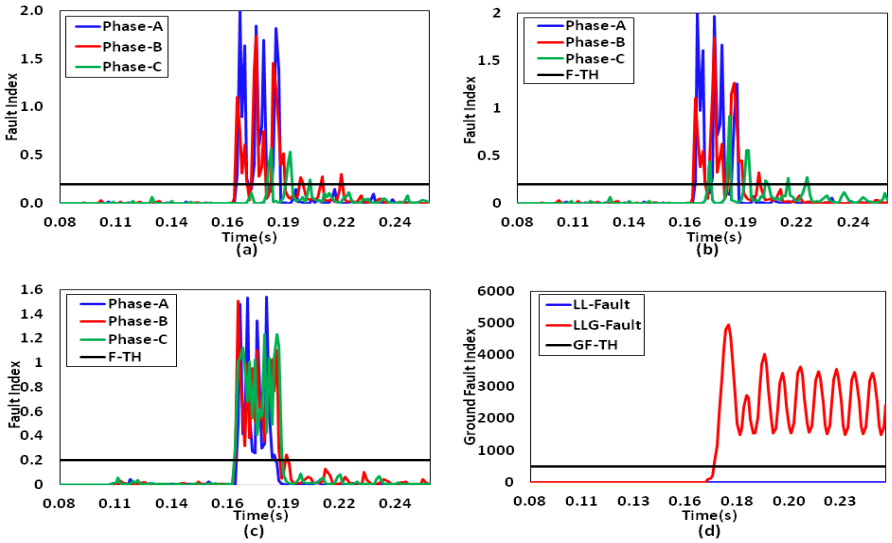

FIGURE 8. Plots for Index w.r.t. time: (a) AB Fault, (b) ABG Fault, (c) ABCG Fault (d) G-FI.

TABLE 3. Parameters used for variation in case studies.

S.No	Parameters	Range of Variation
1	Fault Location (FL)	0-300 kms, in steps of 30 kms, FIA=0° and FIm=0 Ω.
2	Fault Incidence Angle (FIA)	0^0-180^0 in steps of 30^0, FL=150 km from bus-1 and FIm=0 Ω.
3	Fault Impedance (FIm)	0-100 Ω, FL=40 km from bus-1 and FIA=0°
4	Noise Contamination	10-40 dB, in steps of 10 dB, FL=150 km from bus-1, FIm=0 Ω and FIA=0°.
5	Load Switching	10% and 20 % load, FL=40 km from bus-1, FIm=0 Ω and FIA=0°.
6	Sampling Frequency	0.96 kHz, 1.92 kHz and 3.84 kHz, FL=40 km from bus-1, FIm=0 Ω and FIA=0°.
7	UPFC Control Strategy	Power flow Control and Voltage Control, FL=150 km from bus-1, FIm=0 Ω and FIA=0°
8	UPFC Location	At middle of the line and at receiving end, FL=150 km from bus-1, FIm=0 Ω and FIA=0°
9.	SCRs and line length	with short-circuit levels of 6,8,10 and 12 and 50km, 135 km and 230 km i.e. short, medium and long transmission lines and
10.	Hybrid System	150 km OH line and 80 km UG cable

- The current data information will be communicated to the other end via communication channel. For the proposed algorithm, the signals/ data of both the ends, are required, for fault index computation and decision making.
- The proposed algorithm will be tolerant for CT effects because of capability of WT for filtering high frequency transients that is why the CTs, used for measurement, are assumed to be ideal.

V. DEMONSTRATION OF THE PROPOSED ALGORITHM

Before application of the proposed algorithm to various fault conditions, the proposed protection method for fault diagnosis has been demonstrated in this section, in Figs. 6–7. The 3-Φ current signals recorded at bus 1 and 2 are shown in Figs. 6 (a) and (b) respectively. The wavelet-based approximate coefficients of the bus-1 &2 currents are plotted in Figs. 6(c) and (d) respectively. The AL coefficients, computed from approximate coefficients are presented in Figs. 7(a) and (b). Then, Fig. 7(c) presented the plot of FI with respect to time, which is calculated by adding AL coefficients of Figs. 7(a) and (b). From this figure, it can be significantly evident that, only phase A has FI value more than the F-TH, thus indicating AG fault.

Deviations in FIs of 3-Φs for AB, ABG and ABCG faults are illustrated in Fig. 8. It is clear from the Figs. 8(a) and (b), those FIs of both A and B phases have greater values than the F-TH hence, detected as two-phase faults (AB & ABG). Further, Fig. 8(c) presented that FIs of all the phases have higher values with respect to the F-TH value; therefore detected as 3-Φ fault. From the Figs. 8(a) and (b) it is clear that developed FIs can't differentiate between LL and LLG because under both the cases there is no significant changes in the values of FIs.

In Fig. 8 (d), plotted the G-FI w.r.t. time for LL and LLG faults. It is evident by the results that G-FI has greater values with respect to the GF-TH for the faults associated with ground and vice-versa.

VI. CASE STUDIES

The performance of proposed technique is validated for variety of outages under various conditions which are illustrated in Table-3.

A. VARIATION OF FAULT LOCATION AND FAULT INCIPIENT ANGLE (FIA)

With variations in fault locations and fault incidence angles, the fault current transients also vary, thus, the developed

TABLE 4. Results for FI variation with varying fault location and FIA for BG Fault.

Angle	0°			30°			60°			90°			120°			150°		
Location	a	b	c	a	b	c	a	b	c	a	b	c	a	b	c	a	b	c
30	0.11	1.39	0.10	0.06	1.12	0.19	0.10	0.80	0.16	0.02	1.15	0.03	0.15	1.72	0.03	0.04	1.31	0.04
60	0.14	0.71	0.04	0.03	1.07	0.13	0.03	0.43	0.17	0.01	0.74	0.10	0.13	1.69	0.02	0.11	1.42	0.01
90	0.15	0.79	0.03	0.08	1.04	0.03	0.05	0.47	0.11	0.01	0.48	0.11	0.07	1.75	0.01	0.05	1.45	0.01
120	0.07	0.67	0.04	0.09	0.83	0.04	0.07	0.66	0.12	0.00	0.50	0.08	0.07	1.77	0.03	0.09	1.43	0.01
150	0.05	0.49	0.02	0.15	1.02	0.04	0.02	0.69	0.11	0.00	0.41	0.08	0.04	1.81	0.02	0.05	1.65	0.01
180	0.12	1.22	0.08	0.01	1.03	0.05	0.01	0.51	0.14	0.00	1.09	0.06	0.02	1.92	0.02	0.09	1.79	0.01
210	0.08	1.03	0.08	0.00	1.04	0.07	0.02	0.61	0.18	0.00	0.96	0.03	0.03	1.97	0.01	0.04	1.91	0.01
240	0.01	0.76	0.07	0.02	1.06	0.08	0.02	0.78	0.15	0.00	0.81	0.02	0.04	2.00	0.01	0.05	1.93	0.02
270	0.08	1.04	0.14	0.09	1.10	0.10	0.03	1.11	0.16	0.00	0.82	0.01	0.05	1.99	0.01	0.01	1.96	0.01

TABLE 5. Results for FI variation with varying fault location and FIA for BC fault.

Angle	0°			30°			60°			90°			120°			150°		
Location	a	b	c	a	b	c	a	b	c	a	b	c	a	b	c	a	b	c
30	0.11	1.02	0.22	0.04	1.18	1.24	0.14	0.68	1.77	0.00	0.90	1.84	0.01	1.68	0.78	0.08	1.45	0.97
60	0.06	1.56	1.14	0.10	1.15	1.23	0.07	0.65	1.78	0.00	1.04	1.88	0.01	1.71	0.90	0.04	1.44	0.95
90	0.06	1.54	1.12	0.17	0.81	1.20	0.13	0.66	1.78	0.00	0.90	1.87	0.02	1.68	0.88	0.03	1.51	0.82
120	0.04	1.40	1.26	0.10	1.11	1.25	0.12	0.66	1.76	0.00	0.82	1.89	0.02	1.63	1.12	0.09	1.49	0.74
150	0.03	1.36	1.24	0.16	0.80	1.20	0.03	0.81	1.78	0.01	0.71	1.90	0.02	1.65	1.50	0.20	1.55	0.39
180	0.06	1.05	1.12	0.09	1.14	1.17	0.02	0.79	1.78	0.00	0.83	1.97	0.01	1.89	1.02	0.07	1.73	0.33
210	0.04	1.05	1.16	0.09	1.10	1.19	0.04	1.02	1.80	0.00	0.79	1.95	0.01	1.80	1.02	0.13	1.90	0.38
240	0.01	1.00	1.18	0.17	1.09	1.20	0.07	1.06	1.76	0.00	0.73	1.92	0.01	1.77	0.87	0.11	1.71	0.83
270	0.07	0.77	1.18	0.10	1.10	1.18	0.06	1.01	1.70	0.02	0.73	1.86	0.01	1.80	0.91	0.02	1.68	1.31

TABLE 6. Results for FI variation with varying fault location and FIA for ACG fault.

Angle	0°			30°			60°			90°			120°			150°		
Location	a	b	c	a	b	c	a	b	c	a	b	c	a	b	c	a	b	c
30	1.92	0.03	1.03	1.83	0.03	1.04	0.60	0.02	1.63	0.85	0.19	1.82	1.24	0.07	1.08	1.38	0.07	0.42
60	1.55	0.03	0.99	1.94	0.02	1.02	0.53	0.01	1.61	0.62	0.06	1.90	1.26	0.05	0.99	1.38	0.06	0.54
90	1.47	0.02	1.02	1.97	0.01	1.05	0.48	0.01	1.59	0.43	0.06	1.92	1.24	0.04	0.99	1.37	0.16	0.80
120	1.51	0.09	1.02	2.00	0.01	1.04	0.43	0.01	1.63	0.56	0.04	1.93	1.24	0.03	1.14	1.39	0.09	1.03
150	1.50	0.07	1.03	1.98	0.01	1.00	0.42	0.01	1.55	0.76	0.03	1.91	0.84	0.02	1.37	1.34	0.09	0.86
180	1.63	0.04	1.00	1.95	0.00	1.04	0.40	0.01	1.52	0.52	0.03	1.97	1.22	0.14	0.97	1.24	0.19	1.00
210	1.53	0.04	0.74	1.87	0.00	0.91	0.38	0.01	1.70	0.35	0.02	1.93	1.23	0.16	1.00	1.26	0.14	0.90
240	1.51	0.02	0.84	1.90	0.00	0.70	0.35	0.01	1.62	0.33	0.03	1.88	0.99	0.17	0.96	1.38	0.14	0.88
270	1.51	0.01	1.04	1.89	0.00	0.69	0.33	0.01	1.53	0.71	0.04	1.77	0.52	0.11	0.90	0.97	0.16	1.00

TABLE 7. Results for FI variation with varying fault location and FIA for ABCG fault.

Angle	0°			30°			60°			90°			120°			150°		
Location	a	b	c	a	b	c	a	b	c	a	b	c	a	b	c	a	b	c
30	1.91	1.62	1.68	1.83	1.68	1.81	1.95	1.67	1.69	1.33	1.68	1.87	1.30	1.64	1.59	1.40	1.43	1.73
60	1.93	1.66	1.69	1.80	1.67	1.76	1.90	1.67	1.75	1.52	1.67	1.89	1.32	1.65	1.69	1.32	1.46	1.69
90	1.96	1.67	1.68	1.83	1.68	1.74	1.99	1.66	1.76	1.50	1.68	1.87	1.36	1.63	1.64	1.41	1.59	1.76
120	1.96	1.65	1.66	1.83	1.62	1.75	1.99	1.66	1.61	1.46	1.66	1.87	1.39	1.61	1.84	1.38	1.59	1.71
150	1.94	1.80	1.69	1.84	1.53	1.70	1.84	1.53	1.70	1.55	1.72	1.72	1.46	1.77	1.64	1.78	1.50	1.68
180	2.00	1.72	1.69	1.91	1.80	1.70	1.68	1.72	1.70	1.38	1.71	1.94	1.49	1.77	1.67	1.28	1.57	1.68
210	1.99	1.69	1.71	1.73	1.66	1.70	1.98	1.73	1.68	1.70	1.71	1.89	1.33	1.71	1.68	1.35	1.74	1.68
240	1.99	1.70	1.70	1.93	1.79	1.70	1.99	1.72	1.69	1.33	1.72	1.84	1.84	1.69	1.66	1.34	1.58	1.68
270	1.93	1.77	1.69	1.81	1.59	1.70	2.00	1.82	1.71	1.43	1.69	1.76	1.37	1.74	1.67	1.62	1.55	1.68

technique has been validated for its robustness with respect to the varying fault locations and FIAs. For this, different types of faults have been simulated at every 30 km for 300 km length of line and FIA is varied in the range of 0° to 180° in the steps of 30°. The results for the above illustrated strategy have been detailed/illustrated in Tables 4–7, in which faults of each category i.e. BG, BC, ACG and ABCG have been considered for the study. In Table-4, FI value, for only B-phase, is more w.r.t. the F-TH, but for A and C phases, its values are very much lower, this signifies the detection and classification of fault as BG fault. Similarly in Table-5, faulty phases are BC only, hence only for these two phases only FI value is more than the F-TH, not for healthy phase i.e. phase A. ACG fault detections and classification can be similarly distinguished in Table-6 and for ABCG fault, fault index variation for varying fault locations and FIAs is presented in Table-7. Thus, from these results/tables, it can be significantly concluded that proposed algorithm is robust for variations of fault locations and FIAs.

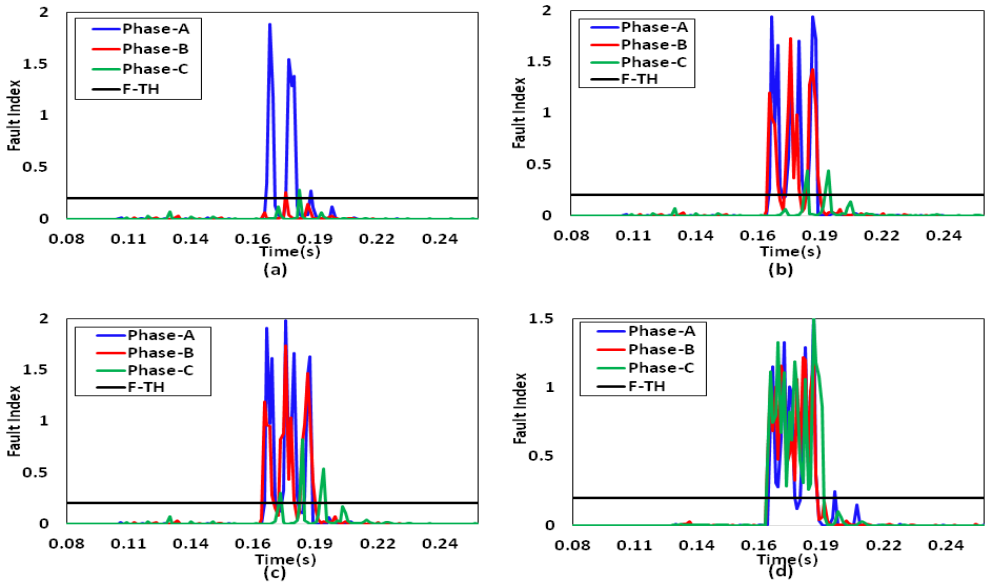

FIGURE 9. Fault detection and classification results for varying FIs: (a) LG Fault (b) LL Fault (c) LLG Fault (d) LLLG Fault.

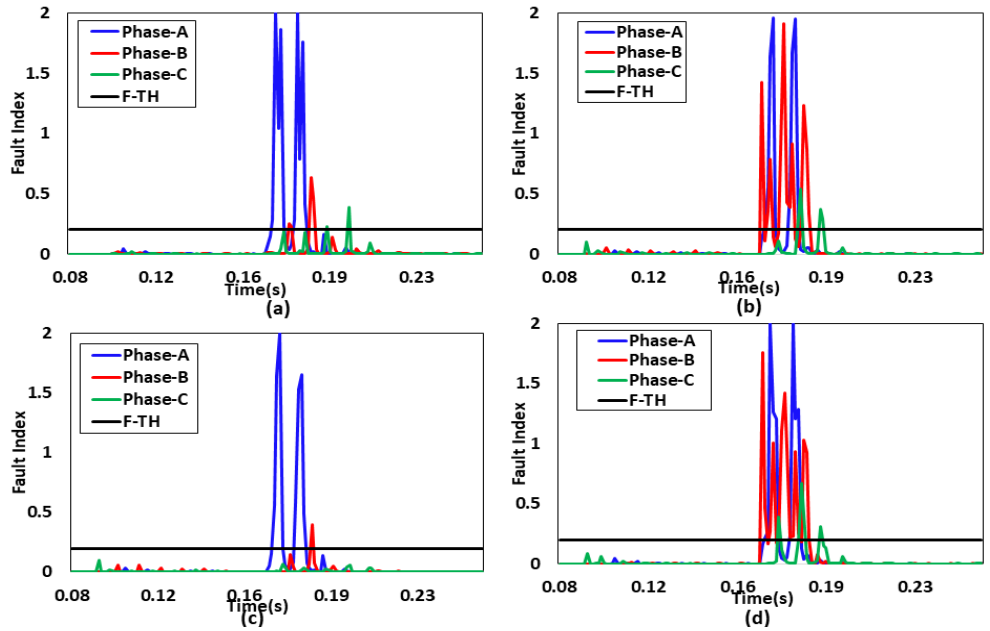

FIGURE 10. Fault diagnosis for different control strategies (a) AG Fault with Power Flow Control (b) AB Fault with Power Flow Control (c) AG Fault with Voltage Control (d) AB Fault with Voltage Control.

B. EFFECT OF HIGH IMPEDANCE FAULTS

The applicability of the developed protection technique is validated by selecting the fault impedances from 0-100Ω under this case study. Fig.9 illustrates the FI variation of all phases with respect to various outages, for the fault impedance of 15Ω. Fig 9(a) presents the phase-A FI which is greater w.r.t. the TH. Further, for remaining phases it is less than the TH for all the impedance values, thus it is diagnosed as AG fault. From Figs. 9(b) and (c), it can be significantly concluded that the values of FIs for A and B phases, are more as compared to the TH but for C it is less. Hence, the faults are diagnosed as AB/LL and ABG/LLG faults, correspondingly. For ABCG fault, the values of FIs for all the phases are greater than the TH as shown in Fig 9(d). Thus, performance of developed algorithm doesn't affected by fault impedance variation.

C. EFFECT OF UPFC OPERATION CONTROL METHOD

The transients developed in the current signals due to faults, will depend on the operation control strategy of UPFC (FACTS device). UPFC uses two control strategies i.e. Power Flow Control and Voltage Control. Hence, the proposed protection method is to be tested for its validation,

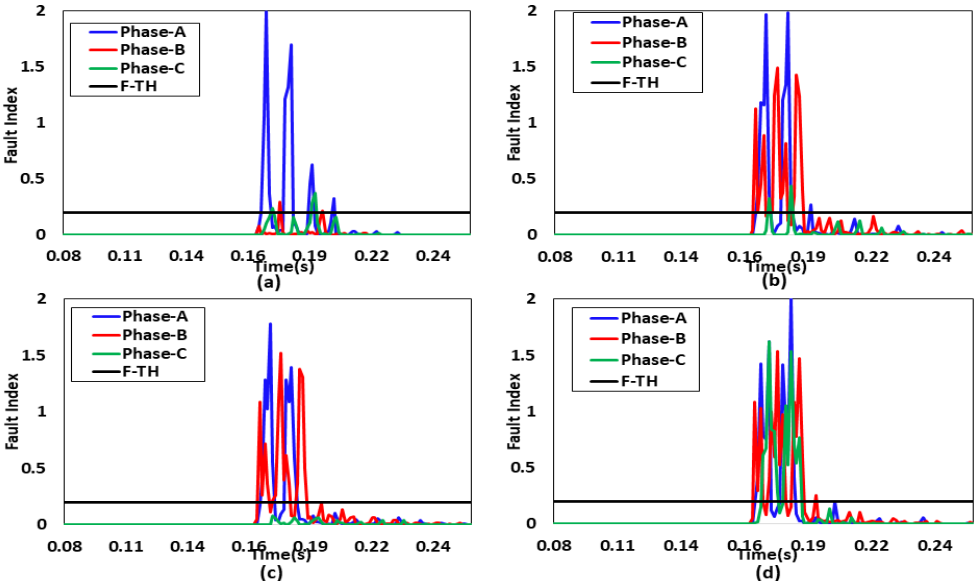

FIGURE 11. Results for fault diagnosis with UPFC connected at bus-2 (a) LG Fault (b) LL Fault (c) LLG Fault (d) LLLG Fault.

with various control strategies of UPFC operation. Figs. 10(a) and (b) presents the results of fault diagnosis (detection and classification) for AG/LG and AB/LL faults, respectively, while UPFC works under Power Flow Control. It can be significantly observed that FI value is greater than the F-TH for faulty phases only. In the similar manner, the Figs. 10(c) and (d) illustrated the fault diagnosis results for AG and AB faults when UPFC works with Voltage Control. In this case also, FI value is greater for faulty phases only and not for healthy phases.

D. UPFC INSTALLED AT RECEIVING END

UPFC location affects the magnitude and transients of bus currents. Hence, the performance of the proposed algorithm is verified by changing the UPFC location to receiving end i.e. at Bus-2. Figs. 11(a)-(d) illustrated the FI deviation of all phases for LG, LL, LLG and LLLG faults, correspondingly. The FI of faulty phases alone, exceed the F-TH. Hence, it is established that the performance of the developed algorithm doesn't get affected by the location of UPFC.

E. PERFORMANCE IN NOISY ENVIRONMENT

In overhead transmission lines, there is chance of noise mixing with current signals due to interference of neighbouring communication circuits. Thus, it is needed to test the proposed protection method with the current signals, which are contaminated with noise. For this purpose the levels of SNRs considered, is 40dB-10dB. Fig. 12 considered various faults and presents the analysis with 10dB white Gaussian noise. Fig 12(a) presents detection and classification result for AG fault, where FI value of faulty phase is more as compared to the TH and for other phases it is lower. Fig 12(b) and (c) show the analysis for AB and ABG faults, for which the FIs for faulty phases i.e. A & B have more value than the TH and for C-phase (healthy phase) has lower value. Fig 12(d) shows results for three phase (ABCG) fault, where all the three phases have higher FIs value than the TH. Thus, it is proved that the proposed algorithm efficiently detects and classifies the faults even in the noisy environment.

F. DISCRIMINATION FROM NON-faulty/SWITCHING TRANSIENTS

In practical/modern power system, non-faulty/switching transients can be developed because of switching of certain power system equipments, like capacitor banks (used for power factor improvement) and inductive/reactor loads (with fluctuation in power demand). But, these switching transients should not be identified as faulty transients, as they are not dangerous for the power system and its equipments. Thus, it is mandatory to check the algorithm for discrimination of non-faulty and faulty transients. For this purpose, a capacitive load of 10% and 20% Q_{rated} has been used for developing capacitive switching transients and an inductive load of 10% and 20% of S_{rated} has been used for creating inductive switching transients. The results for above testing are shown in Fig. 13, from which it can be significantly evident that for switching transients maximum FI value is very less w.r.t. the F-TH, hence in the event of switching transients occurrence, the proposed scheme won't give a false detection for fault.

G. SAMPLING FREQUENCY VARIATION EFFECT

The proposed protection method has been tested with variable sampling frequencies in order to check its accuracy and feasibility to be compatible with different instrumentation equipments. For this purpose, the results have been replicated with

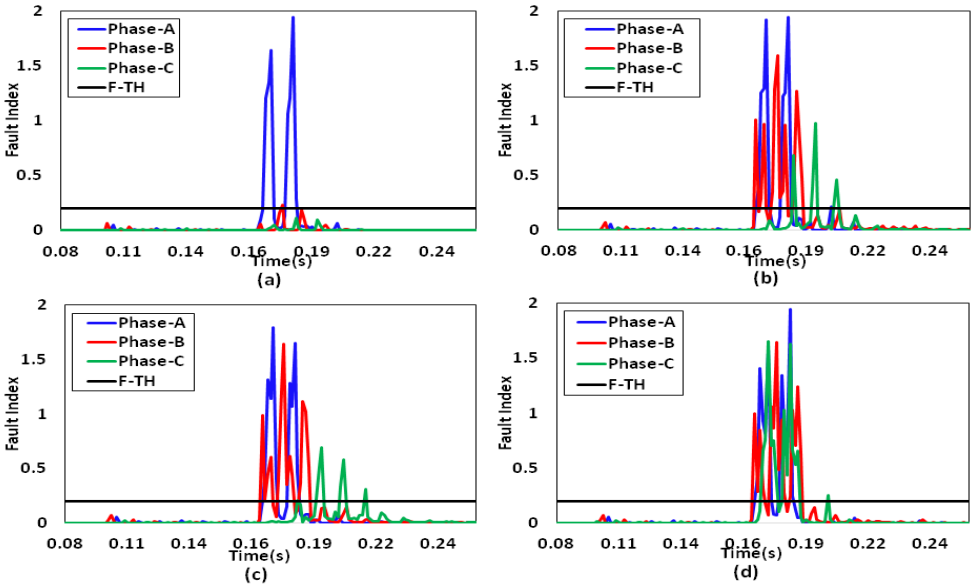

FIGURE 12. Results for fault diagnosis with noise contamination (a) LG Fault (b) LL Fault (c) LLG Fault (d) LLLG Fault.

TABLE 8. Results for sampling frequency variation.

Sampling Frequency	Detection Time	Types of Fault	Fault Index FI_A	Fault Index FI_B	Fault Index FI_C
0.96 kHz	> 5ms	AG	1.33	0.02	0.01
	> 5ms	ABG	1.75	1.34	0.05
	> 5ms	ABCG	1.82	1.56	1.13
1.92 kHz	< 5ms	AG	1.84	0.07	0.05
	< 5ms	ABG	1.58	1.64	0,08
	< 5ms	ABCG	1.58	1.46	1.12
3.84 kHz	< 5ms	AG	1.36	0.01	0.00
	< 5ms	ABG	1.67	1.49	0.03
	< 5ms	ABCG	1.39	1.55	1.38

sampling frequencies of 0.96 kHz, 1.92 kHz and 3.84 kHz and they are presented in table-8. From this table, it is clear that with increase in sampling frequency, the fault detection is still within quarter cycle time, thus no significant effect is seen, while for fault location also the average error remain well within 1%. But when the sampling frequency is reduced, the fault detection time increases for some cases and its accuracy also reduces. Hence, for the proposed protection method the optimum sampling frequency is 1.96 kHz.

H. VARIATION IN SCRs AND LINE LENGTH

In practice, the transmission line relay should work in different conditions, thus the proposed algorithm has been checked on variable line lengths and with sources of variable short circuit levels. For this purpose, the algorithm has been tested for the line lengths of 50km, 135 km and 230 km i.e. short, medium and long transmission lines and with short-circuit levels of 6,8,10 and 12. For all the conditions/cases, the proposed fault detection and classification strategy works very well with 99.99% accuracy.

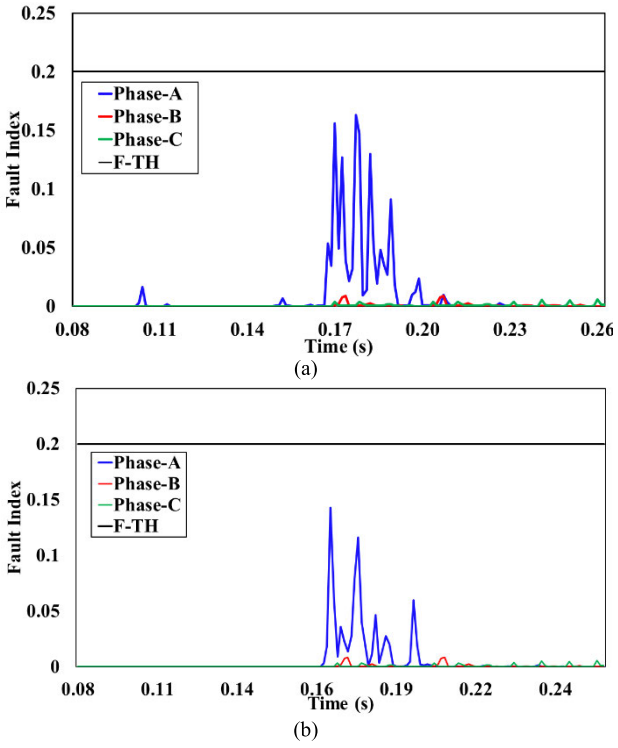

FIGURE 13. Results for Load switching with: (a) 20 % Inductive Load, (b) 20 % Capacitive Load.

I. HYBRID TRANSMISSION SYSTEM

In modern power system, underground cables are also utilized for power transmission networks due to its merits of less maintenance requirement and long-life. But, it is also not possible to install UG cable for whole length due to adverse

TABLE 9. Results for composite (OH line +UG cable) system.

Fault Type	Maximum FI value for fault in OH line		
	Phase-A	Phase-B	Phase-C
AG	1.11	0.04	0.01
ABG	1.89	1.72	0.02
ABCG	0.98	1.23	1.42
Fault Type	**Maximum FI value for fault in UG Cable**		
AG	1.86	0.03	0.06
ABG	1.23	1.61	0.05
ABCG	1.83	1.66	1.71

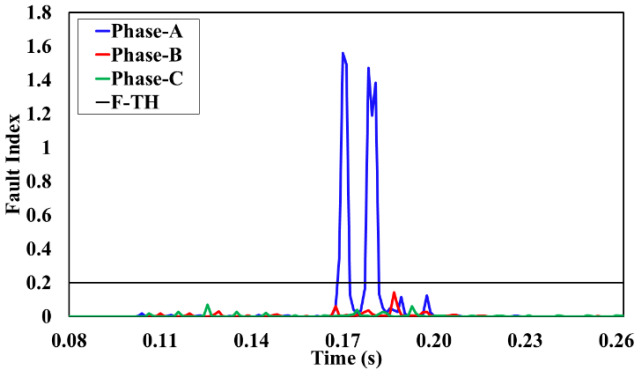

FIGURE 14. AG fault detection for Arcing phenomenon.

geographic conditions, thus hybrid transmission system is used comprising of UG cable and overhead line combination. Thus, for proving the proposed algorithm capability to perform in hybrid systems also, a new system is considered comprising of 150 km OH line and 80 km UG cable [25]. For this system also various faults have been simulated and for all the cases accuracy obtained was 99.99 %, results for the same have been presented in Table-9.

J. EFFECT OF ARCING FAULTS

Arcing Faults arises due to arc formation/phenomenon introducing high impedance in fault current path along with an opposing voltage. This type of fault condition generates transients which are different from those in other short circuit faults, this could alter sensitivity of the relay. Thus, the proposed protection method has been tested for arcing faults also, by creating such condition fault event with a voltage applied opposing fault current flowing through a high impedance path from phase to ground. The results have been replicated in Fig. 14, for this condition with AG fault gives confirmatory results of fault detection and classification. Hence, it can be concluded that arcing faults have no effect on proposed protection scheme.

K. VARIATION OF VOLTAGE LEVELS

In practice, power transmission can be done at different voltage levels (132 kV, 220 kV, 400 kV, 500 kV, 765 kV) depending upon the power demand and physical conditions

TABLE 10. Results for voltage level variation.

Voltage levels	Detection Time	Types of Fault	Phase-A FI	Phase-B FI	Phase-C FI
220 kV	< 5ms	AG	1.47	0.06	0.03
	< 5ms	ABG	1.54	0.98	0.04
	< 5ms	ABCG	1.67	0.93	0.97
400 kV	< 5ms	AG	1.30	0.04	0.01
	< 5ms	ABG	1.49	1.20	0.03
	< 5ms	ABCG	1.87	1.44	0.95
765 kV	< 5ms	AG	1.15	0.02	0.08
	< 5ms	ABG	1.37	1.04	0.03
	< 5ms	ABCG	0.95	1.20	1.12

TABLE 11. Results for TCSC-compensated transmission system.

S.No	Fault Type	Phase-A FI	Phase-B FI	Phase-C FI	Detection Time
1	AG	**1.34**	0.04	0.01	< 5ms
2	BG	0.09	**1.02**	0.07	< 5ms
3	CG	0.00	0.04	**1.30**	< 5ms
4	AB	**1.26**	**0.99**	0.08	< 5ms
5	BC	0.01	**1.85**	**1.20**	< 5ms
6	AC	**0.99**	0.03	**1.43**	< 5ms
7	ABG	**1.68**	**1.49**	0.00	< 5ms
8	BCG	0.01	**1.63**	**1.77**	< 5ms
9	ACG	**1.04**	0.07	**0.84**	< 5ms
10	ABCG	**1.70**	**0.92**	**1.63**	< 5ms

for which transmission systems of different ratings and types can be utilised. For every transmission system to be used, their protection is also a mandatory requirement for efficient and reliable power supply. Thus, the proposed algorithm has been tested for transmission system with different voltage levels of 220 kV, 400 kV and 765 kV and results are shown in Table-10, which signifies the applicability of proposed algorithm for systems with different voltage levels.

L. SERIES COMPENSATED SYSTEM

For establishing the robustness of the proposed algorithm, it has also been tested with series compensated transmission system with Thyristor Controlled Series Capacitor (TCSC) as compensating device. The results for fault analysis of proposed algorithm with TCSC compensated system have been presented in table-11, which establishes the validity of proposed protection scheme for series compensated system also.

VII. LOCATION OF FAULT

Table-12 demonstrates the fault location estimation results using proposed ANN, from which it can be clearly concluded that the peak and mean error, for location of faults, are 1.60% and 0.72%, respectively.

TABLE 12. Estimation of fault location.

S.No	Fault-type	Actual Location	ANN Location	% Error
1	Phase-A to G	42	37.86	1.38
2	Phase-A to G	101	100.54	0.15
3	Phase-A to G	174	171.26	0.91
4	Phase-A to G	231	230.17	0.28
5	Phase-B to G	42	46.63	1.54
6	Phase-B to G	101	101.07	0.02
7	Phase-B to G	174	175.16	0.39
8	Phase-B to G	231	231.20	0.07
9	Phase-C to G	42	40.73	0.42
10	Phase-C to G	101	101.61	0.20
11	Phase-C to G	174	174.12	0.04
12	Phase-C to G	231	229.42	0.53
13	Phase-A to B	42	40.76	0.41
14	Phase-A to B	101	101.72	0.24
15	Phase-A to B	174	170.47	1.18
16	Phase-A to B	231	230.24	0.25
17	Phase-B to C	42	42.28	0.09
18	Phase-B to C	101	98.83	0.72
19	Phase-B to C	174	170.95	1.02
20	Phase-B to C	231	228.74	0.75
21	Phase-A to C	42	39.62	0.79
22	Phase-A to C	101	100.93	0.02
23	Phase-A to C	174	174.25	0.08
24	Phase-A to C	231	227.03	1.32
25	Phases-AB to G	42	39.29	0.90
26	Phases-AB to G	101	101.61	0.20
27	Phases-AB to G	174	176	0.67
28	Phases-AB to G	231	230.52	0.16
29	Phases-BC to G	42	39.23	0.92
30	Phases-BC to G	101	101.16	0.05
31	Phases-BC to G	174	176.57	0.86
32	Phases-BC to G	231	227.95	1.02
33	Phases-AC to G	42	42.84	0.60
34	Phases-AC to G	101	100.83	0.06
35	Phases-AC to G	174	168.61	1.80
36	Phases-AC to G	231	227.85	1.05
37	Phases-ABC to G	42	45.13	1.04
38	Phases-ABC to G	101	102.35	0.45
39	Phases-ABC to G	174	176.35	0.78
40	Phases-ABC to G	231	231.75	0.25

TABLE 13. Performance study of proposed transmission system.

Fault Type	A		B		C	
	Without UPFC	With UPFC	Without UPFC	With UPFC	Without UPFC	With UPFC
AG	1.18	1.20	0.05	0.06	0.01	0.01
BG	0.06	0.09	1.38	1.14	0.01	0.01
CG	0.10	0..11	0.01	0.01	0.90	0.95
AB	1.37	1.25	0.98	1.00	0.01	0.01
BC	0.01	0.01	1.43	1.38	0.96	0.95
AC	1.42	1.49	0.01	0.01	0.74	0.76
ABG	1.28	1.31	1.02	0.98	0.01	0.01
BCG	0.04	0.05	1.40	1.10	0.68	0.78
ACG	1.50	1.46	0.03	0.04	0.73	0.66
ABC	1.36	1.44	0.86	0.99	1.09	1.07

VIII. PERFORMANCE STUDY IN UPFC ABSENCE

In practical power system, sometimes due to maintenance or outage the FACTS devices are disconnected from the system, but in this scenario also the protection algorithm should be active and perform well. Thus, the proposed algorithm is needed to be tested in absence of UPFC, from the system.

TABLE 14. Fault location for system without UPFC.

S.No	Fault-type	Actual Location	ANN Location	% Error
1	AG	35	36.84	0.61
2	BG	84	81.52	0.82
3	CG	105	105.55	0.18
4	AB	75	78.90	1.30
5	BC	150	149.61	0.39
6	AC	268	265.32	0.89
7	ABG	69	70.00	0.33
8	BCG	187	185.98	0.34
9	ACG	250	253.12	1.04
10	ABCG	53	53.69	0.23

For this purpose, UPFC has been disconnected from the system and results for fault diagnosis have been computed. Tables 13-14 compare the results of WAN technique for protection of system in presence and absence of UPFC. From this table, the FIs of faulty phases remain higher as compared to the TH, both in the presence and absence of UPFC. The realization of the utilized ANN is computed in the absence of UPFC for all types of faults and outcomes are presented in Table-13-14. Thus, it is proved that the developed algorithm efficiently works with and without UPFC.

IX. COMPARATIVE STUDY

For showing the superiority of the developed Wavelet-Alienation-Neural (WAN) based protection technique, comparison has been done for proposed algorithm w.r.t. protection schemes proposed in the literature in Table-15, with following considerations:

- For comparison, selection of those papers/ research works was done, having UPFC compensated system used for fault analysis.
- The comparison has been made mainly regarding the performance parameters of the algorithms like average error, fault detection time or operating speed, data used and achieved/performed tasks (detection, classification and location).
- For checking the robustness of the comparing algorithms, consideration of various attributes have been done like variation of location, incidence angle, impedance, sampling frequency, impedance, UPFC control strategy, UPFC location and effect of noise.

From Table-15, it can be clearly concluded that:

- It is absolute protection scheme which is capable of detection, classifying and location the fault.
- The proposed algorithm has least fault detection time i.e. < 5 ms.
- It made use of only post- quarter cycle data for the analysis.
- It is more robust as compared to the other algorithms by considering many case studies.
- The accuracy/ efficiency in fault detection and classification was $> 99\%$.
- The average error in fault location was only $< 1\%$.

TABLE 15. Comparative study (C-Considered and NC-Not Considered).

References	[9]	[5]	[11]	[16]	[6]	[7]	[10]	[15]	[12]	[14]	Proposed algorithm
Technique used	Cross-diff. protection using FDST	Decision tree	FDOST	Differential relaying using WT and DFT	Differential equation based	Quadratic Equation /Optimization based	Sparse S-transform	Wavelet entropy based	Hyperbolic ST and SVM based	Fuzzy-Wavelet approach	WAN
Fault detection time (ms)	> 5	> 5	> 5	> 5	> 5	-	-	-	-	> 5	< 5
Average Error (%)	-	-	>1 %	< 1%	> 2%	0.81%	>2%	-	0.90 %	>1%	0.72%
Sampling Frequency (Hz)	3.84k	1 K	3k	20k	1k	-	3.84k	10 k	6k	-	1.92k
Effect of high impedance faults	C	C	C	C	C	C	C	NC	C	C	C
Effect of Fault Incidence Angle	C	C	C	C	NC	NC	NC	NC	C	C	C
Effect of Fault Location	C	C	C	C	C	C	C	NC	C	C	C
Fault Classification	C	C	C	C	NC	NC	NC	C		C	C
Fault Location Estimation	C	NC	NC	NC	C	C	C	NC	C	C	C
Effect of Control Strategy	C	C	C	NC	C	NC	C	NC	C	NC	C
Effect of UPFC location	NC	NC	NC	NC	NC	NC	NC	C	NC	NC	C
Effect of Noise	C	NC	C	NC	NC	NC	NC	NC	C	NC	C
Effect of Non-Faulty Transients	NC	C	NC	NC	NC	NC	NC	NC	NC	NC	C
Effect of varying source parameters	NC	NC	C	C	NC	NC	NC	NC	NC	NC	C
Effect of Sampling Frequency	NC	NC	NC	NC	NC	NC	NC	NC	C	NC	C
Hybrid system	NC	NC	NC	NC	NC	NC	NC	NC	NC	NC	C
Arcing fault	NC	NC	NC	NC	NC	NC	NC	NC	NC	NC	C
Data Used	-	1 cycle	1 cycle	-	Half cycle	-	1 cycle	-	1 cycle	Half cycle	Quarter cycle

X. CONCLUSION

A WAN depended protection technique is developed for detecting, classifying and locating the faulty conditions on transmission line, operating with UPFC. Approximate decomposition of current signals, computed over the span of quarter cycle, are compared in terms of AL coefficients to detect and classify faults. Evaluation of fault position is performed by ANN. The average error at fault position is calculated to be 0.72%. The absence of UPFC, variations in fault positions, impedance and incidence angle are found to have no impact on the performance of developed algorithm. Thus, the developed technique can be used for protecting the TL, integrated with UPFC, successfully.

REFERENCES

[1] X. Zhou, H. Wang, R. K. Aggarwal, and P. Beaumont, "Performance evaluation of a distance relay as applied to a transmission system with UPFC," *IEEE Trans. Power Del.*, vol. 21, no. 3, pp. 1137–1147, Jul. 2006.

[2] P. K. Dash, A. K. Pradhan, and G. Panda, "Distance protection in the presence of unified power flow controller," *Electric Power Syst. Res.*, vol. 54, no. 3, pp. 189–198, Jun. 2000.

[3] S. Jamali, A. Kazemi, and H. Shateri, "Modified distance protection in presence of UPFC on a transmission line," in *Proc. 9th IET Int. Conf. AC DC Power Transmiss. (ACDC)*, 2010, p. 11.

[4] R. Dubey, S. R. Samantaray, B. K. Panigrahi, and G. V. Venkoparao, "Adaptive distance relay setting for parallel transmission network connecting wind farms and UPFC," *Int. J. Electr. Power Energy Syst.*, vol. 65, pp. 113–123, Feb. 2015.

[5] S. R. Samantaray, "Decision tree-based fault zone identification and fault classification in flexible AC transmissions-based transmission line," *IET Gener., Transmiss. Distrib.*, vol. 3, no. 5, pp. 425–436, May 2009.

[6] S. R. Samantaray, L. N. Tripathy, and P. K. Dash, "Differential equation-based fault locator for unified power flow controller-based transmission line using synchronised phasor measurements," *IET Gener., Transmiss. Distrib.*, vol. 3, no. 1, pp. 86–98, 2009.

[7] M. G. Ahsaee and J. Sadeh, "New fault-location algorithm for transmission lines including unified power-flow controller," *IEEE Trans. Power Del.*, vol. 27, no. 4, pp. 1763–1771, Oct. 2012.

[8] J. M. Kumar, S. R. Samantaray, and L. Tripathy, "Decision tree-induced fuzzy rule-based differential relaying for transmission line including unified power flow controller and wind-farms," *IET Gener., Transmiss. Distrib.*, vol. 8, no. 12, pp. 2144–2152, no. 2014.

[9] L. N. Tripathy, P. K. Dash, and S. R. Samantaray, "A new cross-differential protection scheme for parallel transmission lines including UPFC," *IEEE Trans. Power Del.*, vol. 29, no. 4, pp. 1822–1830, Aug. 2014.

[10] L. Tripathy, S. R. Samantaray, and P. K. Dash, "Sparse S-transform for location of faults on transmission lines operating with unified power flow controller," *IET Gener., Transmiss. Distrib.*, vol. 9, no. 15, pp. 2108–2116, 2015.

[11] Z. Moravej, M. Pazoki, and M. Khederzadeh, "New pattern-recognition method for fault analysis in transmission line with UPFC," *IEEE Trans. Power Del.*, vol. 30, no. 3, pp. 1231–1242, Jun. 2015.

[12] Z. Moravej, M. Pazoki, and M. Khederzadeh, "New smart fault locator in compensated line with UPFC," *Int. J. Electr. Power Energy Syst.*, vol. 92, pp. 125–135, Nov. 2017.
[13] L. N. Tripathy, S. R. Samantaray, and P. K. Dash, "A fast time–frequency transform based differential relaying scheme for UPFC based double-circuit transmission line," *Int. J. Elect. Power Energy Syst.*, vol. 77, pp. 404–417, May 2016.
[14] R. K. Goli, A. Gafoor Shaik, and S. S. Tulasi Ram, "A transient current based double line transmission system protection using fuzzy-wavelet approach in the presence of UPFC," *Int. J. Electr. Power Energy Syst.*, vol. 70, pp. 91–98, Sep. 2015.
[15] A. M. El-Zonkoly and H. Desouki, "Wavelet entropy based algorithm for fault detection and classification in FACTS compensated transmission line," *Int. J. Electr. Power Energy Syst.*, vol. 33, no. 8, pp. 1368–1374, Oct. 2011.
[16] L. N. Tripathy, M. K. Jena, and S. R. Samantaray, "Differential relaying scheme for tapped transmission line connecting UPFC and wind farm," *Int. J. Electr. Power Energy Syst.*, vol. 60, pp. 245–257, Sep. 2014.
[17] M. E. Masoud and M. M. A. Mahfouz, "Protection scheme for transmission lines based on alienation coefficients for current signals," *IET Gener., Transmiss. Distrib.*, vol. 4, no. 11, pp. 1236–1244, 2010.
[18] S. A. Gafoor, S. K. Yadav, P. Prashanth, and T. V. Krishna, "Transmission line protection scheme using wavelet based alienation coefficients," in *Proc. IEEE Int. Conf. Power Energy (PECon)*, Dec. 2014, pp. 32–36.
[19] B. Rathore and A. G. Shaik, "Fault detection and classification on transmission line using wavelet based alienation algorithm," in *Proc. IEEE Innov. Smart Grid Technol.-Asia (ISGT ASIA)*, Nov. 2015, pp. 1–6.
[20] B. Rathore and A. G. Shaik, "Alienation based fault detection and classification in transmission lines," in *Proc. Annu. IEEE India Conf. (INDICON)*, Dec. 2015, pp. 1–6.
[21] B. Rathore and A. G. Shaik, "Wavelet-alienation based transmission line protection scheme," *IET Gener., Transmiss. Distrib.*, vol. 11, no. 4, pp. 995–1003, Mar. 2017.
[22] O. P. Mahela, A. Saraswat, S. K. Goyal, S. Jhajharia, B. Rathore, and S. R. Ola Wigner, "Wigner distribution function and alienation coefficient-based transmission line protection scheme," *IET Gener., Transmiss. Distrib.*, vol. 14, no. 10, pp. 1842–1853, 2020.
[23] S. R. Ola, A. Saraswat, S. K. Goyal, and S. K. Jhajharia, "A protection scheme for a power system with solar energy penetration," *Appl. Sci.*, vol. 10, no. 4, p. 156, 2020, doi: 10.3390/app10041516.
[24] S. Ram Ola, A. Saraswat, S. K. Goyal, V. Sharma, B. Khan, O. P. Mahela, H. Haes Alhelou, and P. Siano, "Alienation coefficient and Wigner distribution function based protection scheme for hybrid power system network with renewable energy penetration," *Energies*, vol. 13, no. 5, p. 1120, Mar. 2020, doi: 10.3390/en13051120.
[25] B. Patel, "A new FDOST entropy based intelligent digital relaying for detection, classification and localization of faults on the hybrid transmission line," *Electr. Power Syst. Res.*, vol. 157, pp. 39–47, Apr. 2018.

BHUVNESH RATHORE received the B.E. and M.E. degrees in electrical engineering from the MBM Engineering College, Jodhpur, in 2010 and 2013, respectively, and the Ph.D. degree in electrical engineering from the Indian Institute of Technology Jodhpur, India, in 2019. He is currently working as a Lecturer with the Department of Electrical and Electronics Engineering, MBM Engineering College. He has authored 12 research articles all in peer-reviewed SCI indexed journals and international IEEE conferences. His research interests include development of power system protection algorithms using multi-resolution analysis, such as wavelet transform and S-transform for transmission systems. The courses taught by him include power system protection, electrical machines, power system, and basic electrical engineering.

OM PRAKASH MAHELA (Senior Member, IEEE) was born in Sabalpura, Kuchaman, Rajasthan, India, in 1977. He received the B.E. degree in electrical engineering from the College of Technology and Engineering, Udaipur, India, in 2002, the M.Tech. degree in electrical engineering from Jagannath University, Jaipur, India, in 2013, and the Ph.D. degree in electrical engineering from IIT Jodhpur, India, in 2018. From 2002 to 2004, he was an Assistant Professor with the Rajasthan Institute of Engineering and Technology, Jaipur. Since July 2004, he has been an Assistant Engineer with Rajasthan Rajya Vidyut Prasaran Nigam Ltd., India. He has authored more than 100 articles. His research interests include power quality, power system planning, and grid integration of renewable energy sources, FACTS devices, transmission line protection, and condition monitoring. He was a recipient of the Gold Medal, in 2013, and the IEEE Conference Best Research Paper Award, in 2018.

BASEEM KHAN (Member, IEEE) received the Bachelor of Engineering degree in electrical engineering from Rajiv Gandhi Technological University, Bhopal, India, in 2008, and the Master of Technology and Doctor of Philosophy degrees in electrical engineering from the Maulana Azad National Institute of Technology, Bhopal, in 2010 and 2014, respectively. He is currently working as a Faculty Member with Hawassa University, Ethiopia. His research interests include power system restructuring, power system planning, smart grid technologies, meta-heuristic optimization techniques, reliability analysis of renewable energy systems, power quality analysis, and renewable energy integration.

SANJEEVIKUMAR PADMANABAN (Senior Member, IEEE) received the bachelor's degree in electrical engineering from the University of Madras, Chennai, India, in 2002, the master's degree (Hons.) in electrical engineering from Pondicherry University, Puducherry, India, in 2006, and the Ph.D. degree in electrical engineering from the University of Bologna, Bologna, Italy, in 2012.

From 2012 to 2013, he was an Associate Professor with VIT University. He joined the National Institute of Technology, India, as a Faculty Member, in 2013. He was invited as a Visiting Researcher with the Department of Electrical Engineering, Qatar University, Doha, Qatar, funded by the Qatar National Research Foundation (Government of Qatar), in 2014. He continued his research activities with the Dublin Institute of Technology, Dublin, Ireland, in 2014. From 2016 to 2018, he was an Associate Professor with the Department of Electrical and Electronics Engineering, University of Johannesburg, Johannesburg, South Africa. Since 2018, he has been a Faculty Member with the Department of Energy Technology, Aalborg University, Esbjerg, Denmark. He has authored more than 300 scientific articles. He is a Fellow of the Institution of Engineers, India, the Institution of Electronics and Telecommunication Engineers, India, and the Institution of Engineering and Technology, U.K. He was a recipient of the Best Paper cum Most Excellence Research Paper Award from IETSEISCON' 13, IET-CEAT'16, IEEE-EECSI'19, and IEEE-CENCON'19, and five Best Paper Awards from ETAEERE'16 sponsored Lecture Notes in Electrical Engineering, Springer book. He is an Editor/Associate Editor/Editorial Board of refereed journals, in particular the IEEE Systems Journal, the IEEE Transactions on Industry Applications, IEEE Access, *IET Power Electronics*, and the *International Transactions on Electrical Energy Systems* (Wiley), and the Subject Editor of *IET Renewable Power Generation*, *IET Generation, Transmission & Distribution*, and Facts journal (Canada).